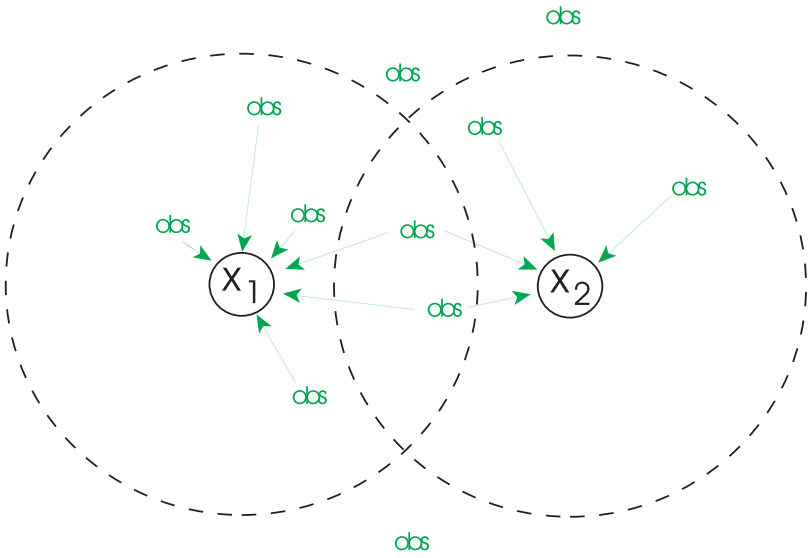

Figure 9. One OI data selection strategy is to assume that each analysis point is only sensitive to observations located in a small vicinity. Therefore, the observations used to perform the analysis at two neighbouring points x_1 or x_2 may be different, so that the analysis field will generally not be continuous in space. The cost of the analysis increases with the size of the selection domains.

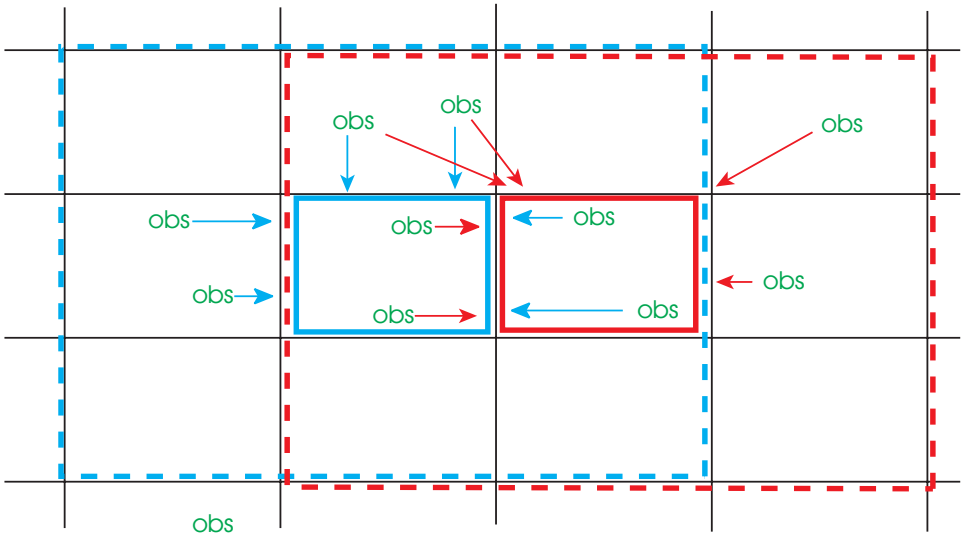

Figure 10. A slightly more sophisticated and more expensive OI data selection is to use, for all the points in an analysis box (black rectangle), all observations located in a bigger selection box (dashed rectangle), so that most of the observations selected in two neighbouring analysis boxes are identical.

The advantage of OI is its simplicity of implementation and its relatively small cost if the right assumptions can be made on the observation selection.

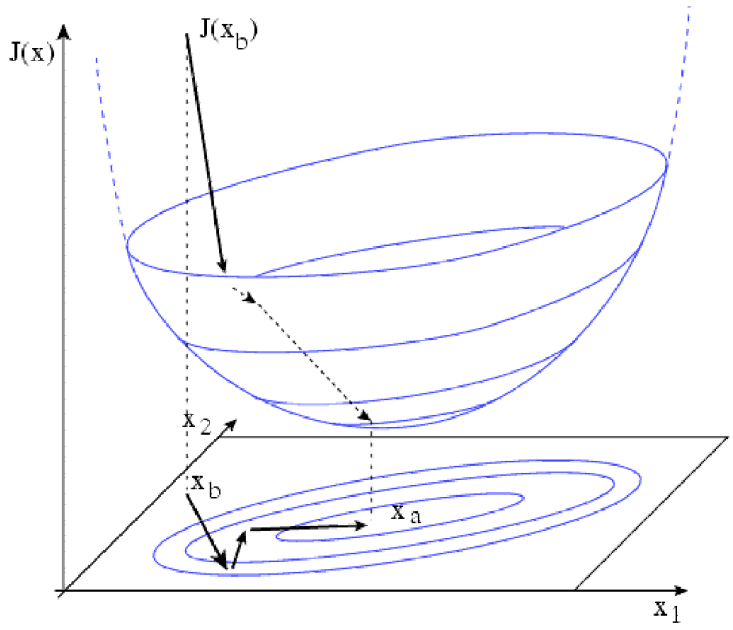

[ECMWF Training Course Notes, 2002]

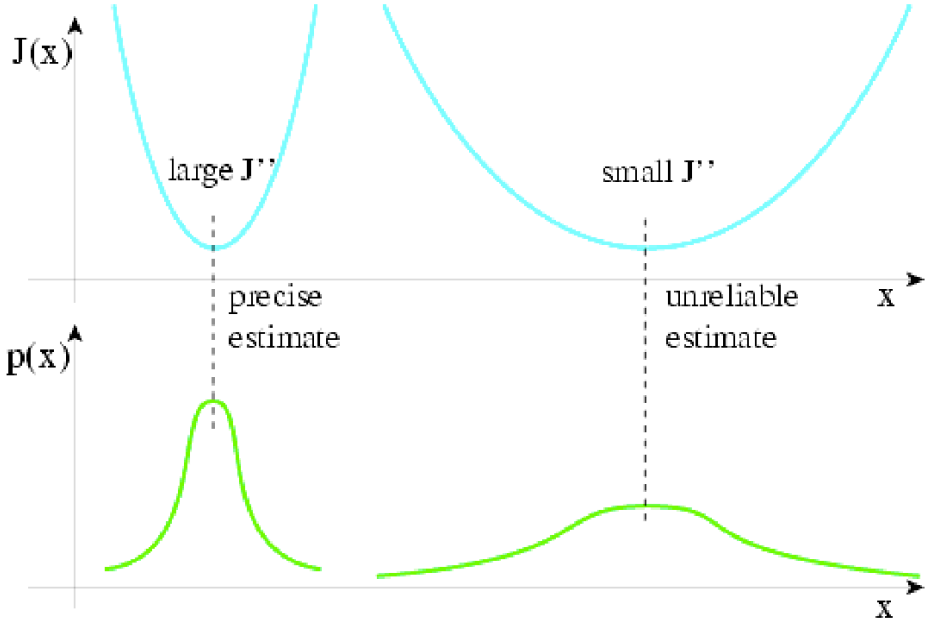

[ECMWF Training Course Notes, 2002]

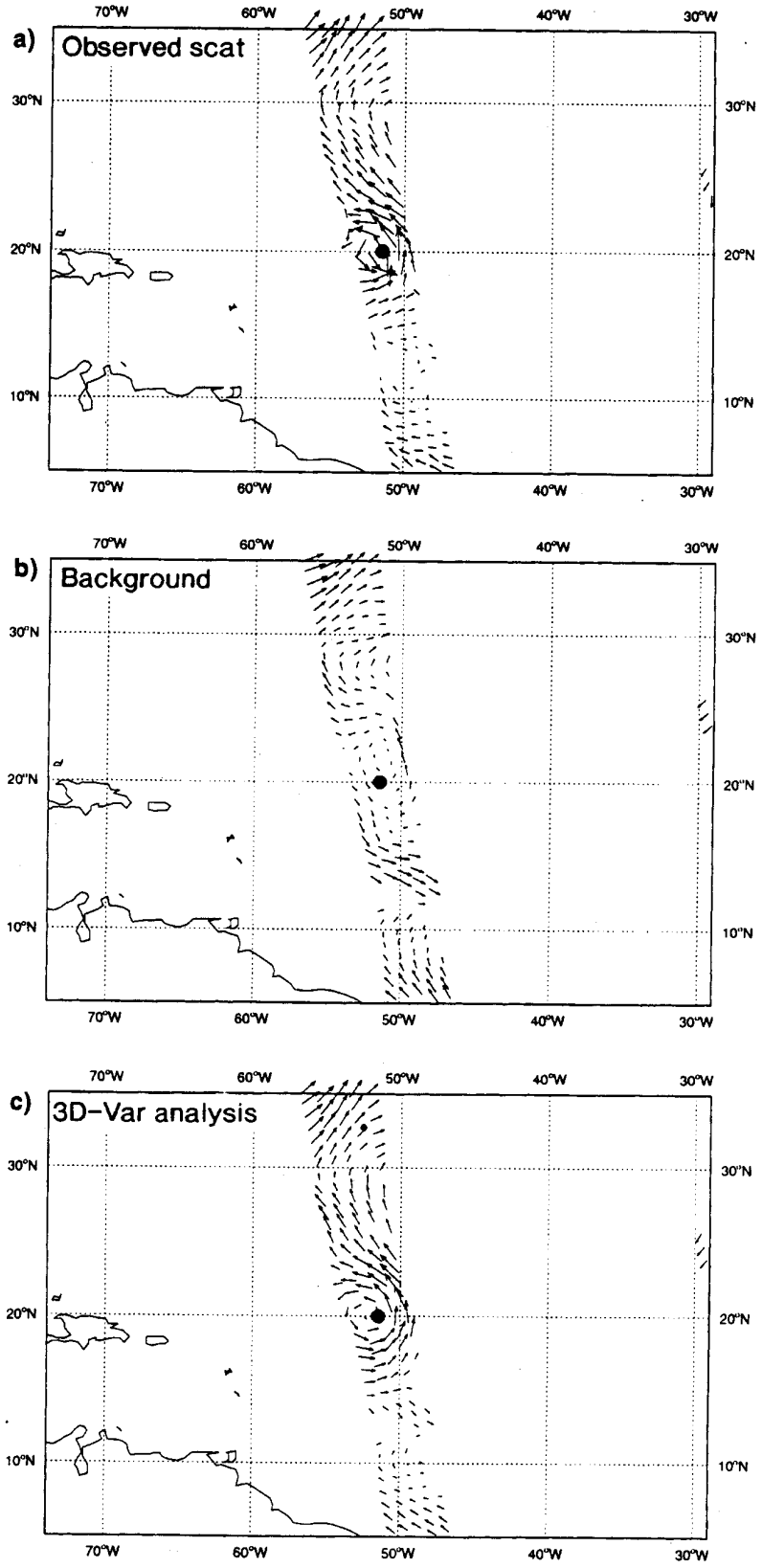

Figure 11. Winds beneath an orbit which passes over tropical cyclone *Karen* located at 20°N, 52°W (large dot) on 31 August 1995: (a) observed by scatterometer; (b) background (six-hour) forecast valid for the same time; (c) 3D-Var analysis. (b) and (c) are interpo;ated to the positions of the scatterometer observations.

Andersson et al. (1998)

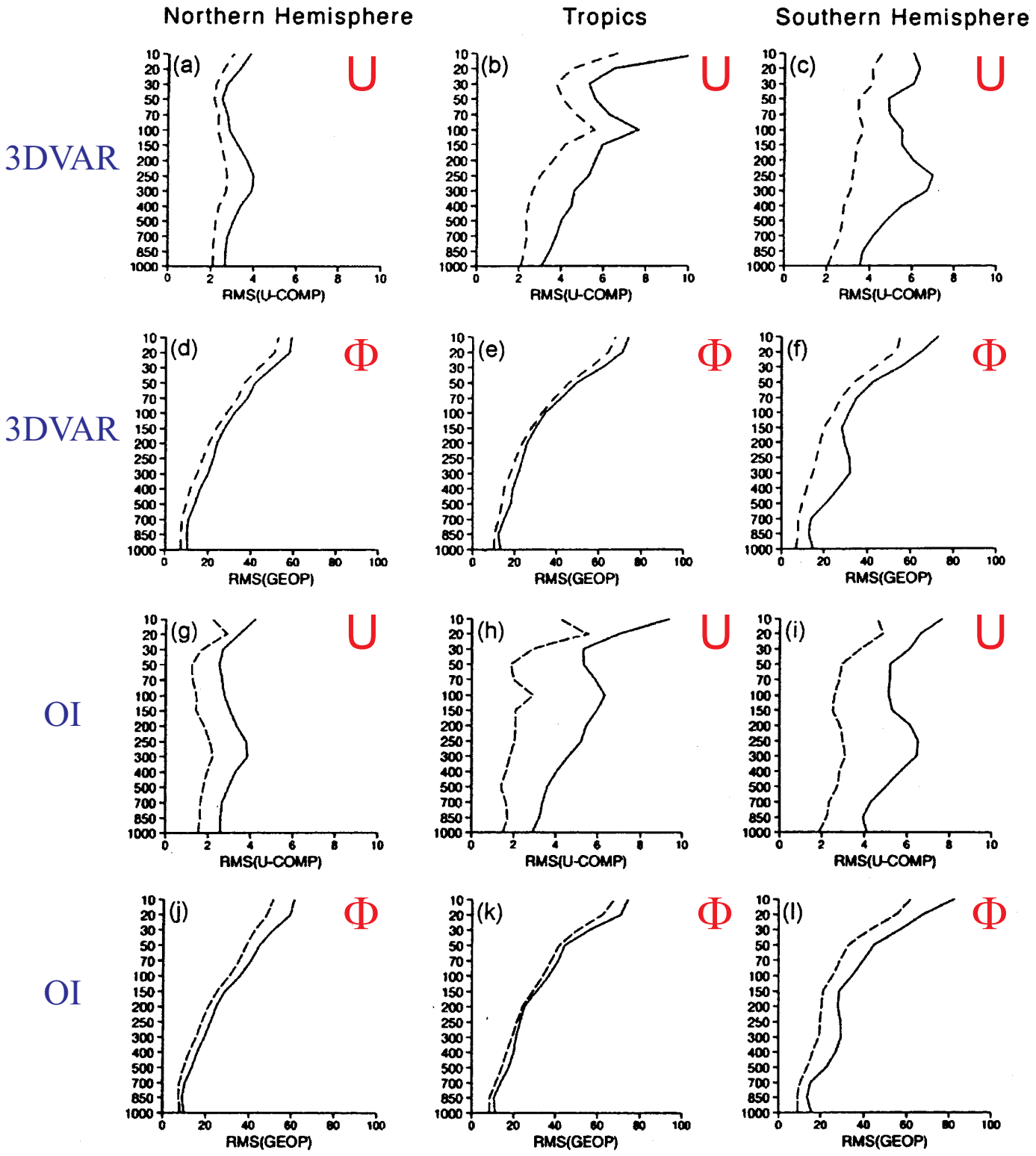

Figure 7. R.m.s. differences at levels from 1000 hPa to 10 hPa for the fourteen-day period 12 UTC 24 August 1995–6 September 1995, between values from all radiosonde data which were used and corresponding values from 3D-Var and OI:

(a) *u* component, 3D-Var, NH; (b) *u* component, 3D-Var, tropics; (c) *u* component, 3D-Var, SH;
(d) geopotential, 3D-Var, NH; (e) geopotential, 3D-Var, tropics; (f) geopotential, 3D-Var, SH;
(g) *u* component, OI, NH; (h) *u* component, OI, tropics; (i) *u* component, OI, SH;
(j) geopotential, OI, NH; (k) geopotential, OI, tropics; (l) geopotential, OI, SH.

NH denotes northern hemisphere north of 20°N, SH denotes southern hemisphere south of 20°S and tropics denotes the region within 20 degrees of the equator. Pecked lines denote observation minus analysis and full lines observation minus background.

Andersson et al. (1998)

3DVAR

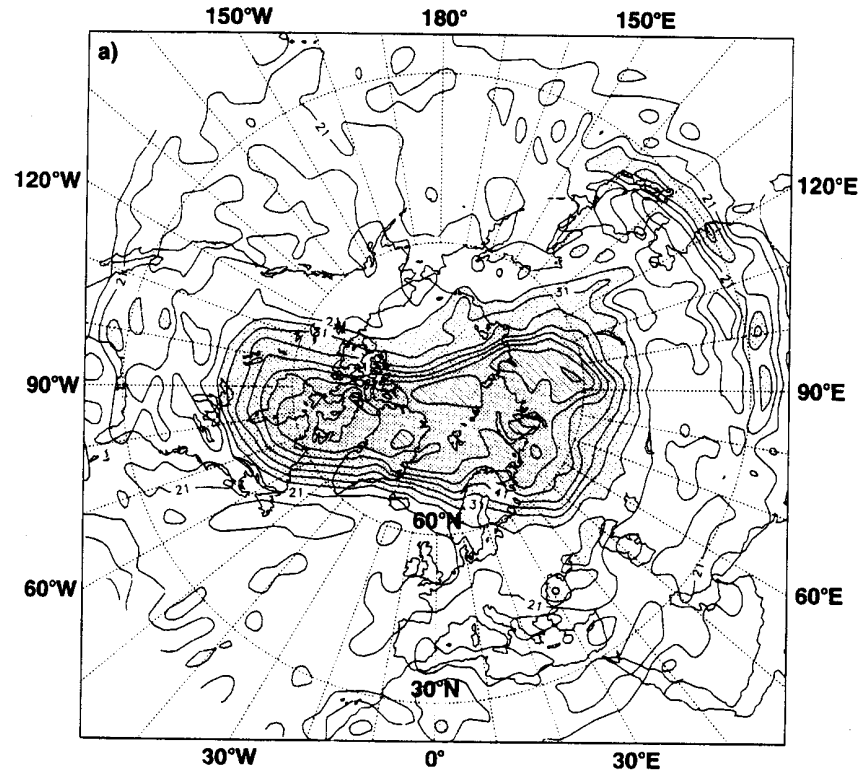

OI

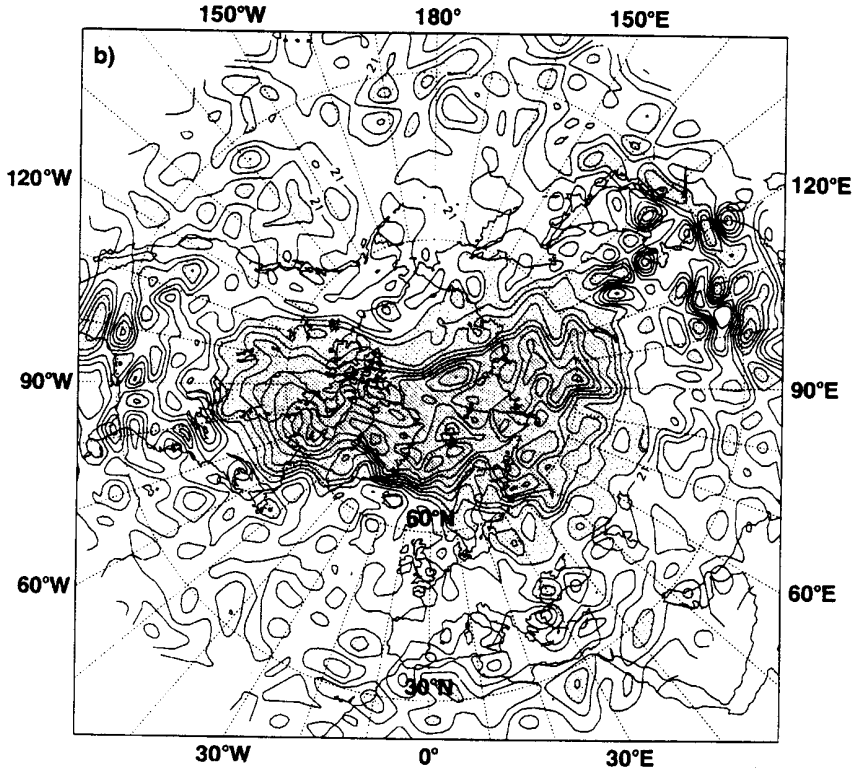

Figure 10. Potential vorticity on the 475 K isentropic surface in northern mid- to high latitudes at 12 UTC 29 January 1996: (a) 3D-Var; (b) OI.

Andersson et al. (1998)

height 500 mb

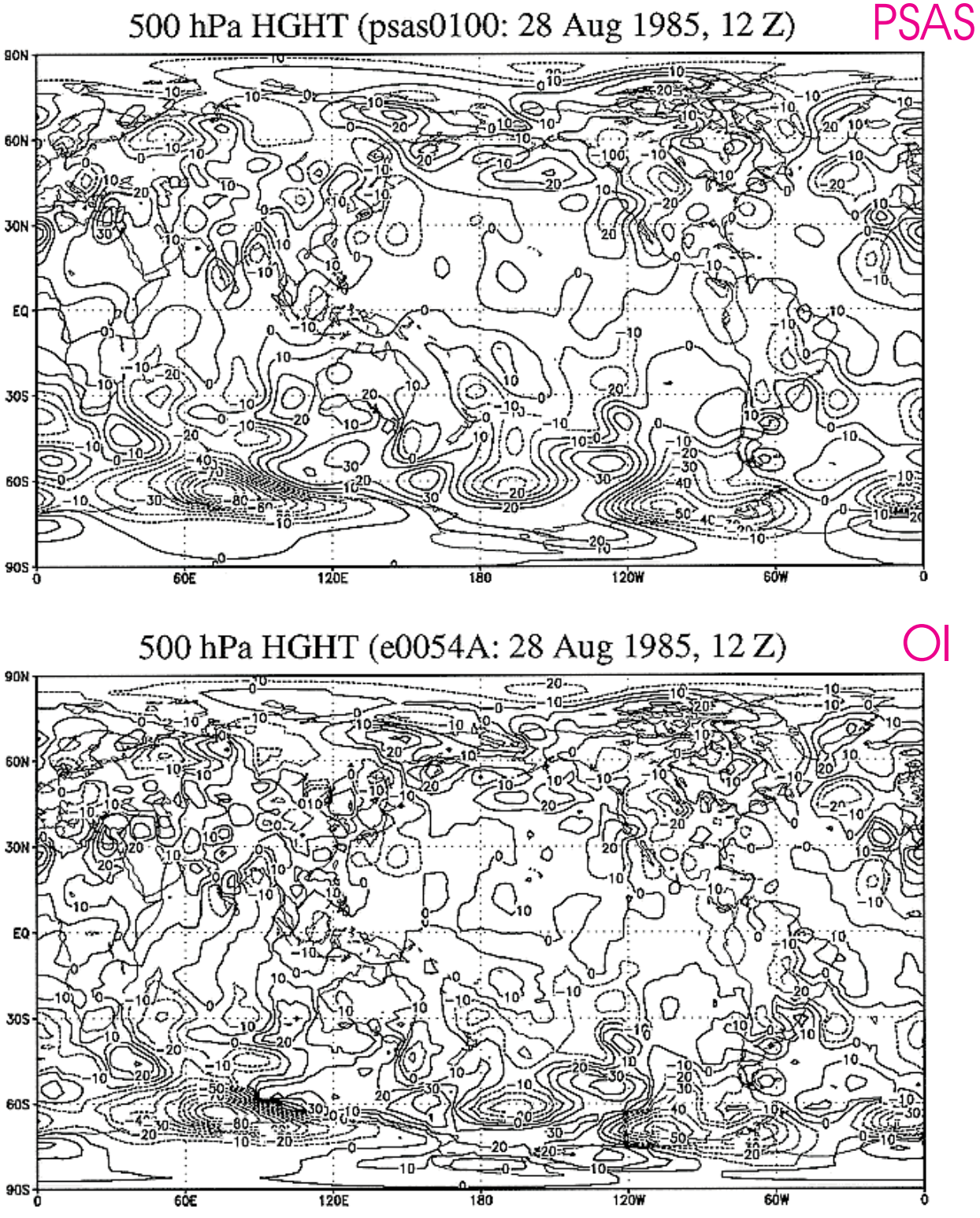

Fig. 2. Height analysis increments at 500 hPa for 1200 UTC 28 August 1985 (case 1) produced with PSAS (top panel) and GEOS-1 OI (bottom panel). Contour interval: 10 m.

Cohn et al. (1998)

Streamfunction 200 mb

PSAS

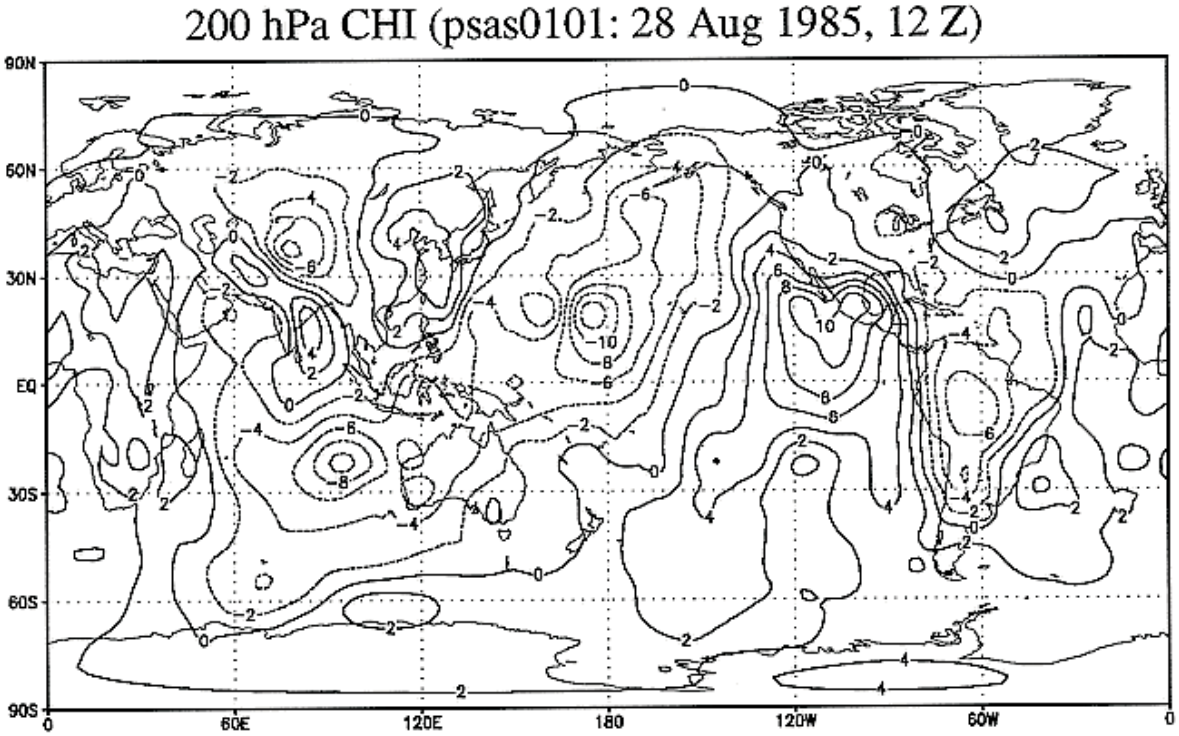

OI

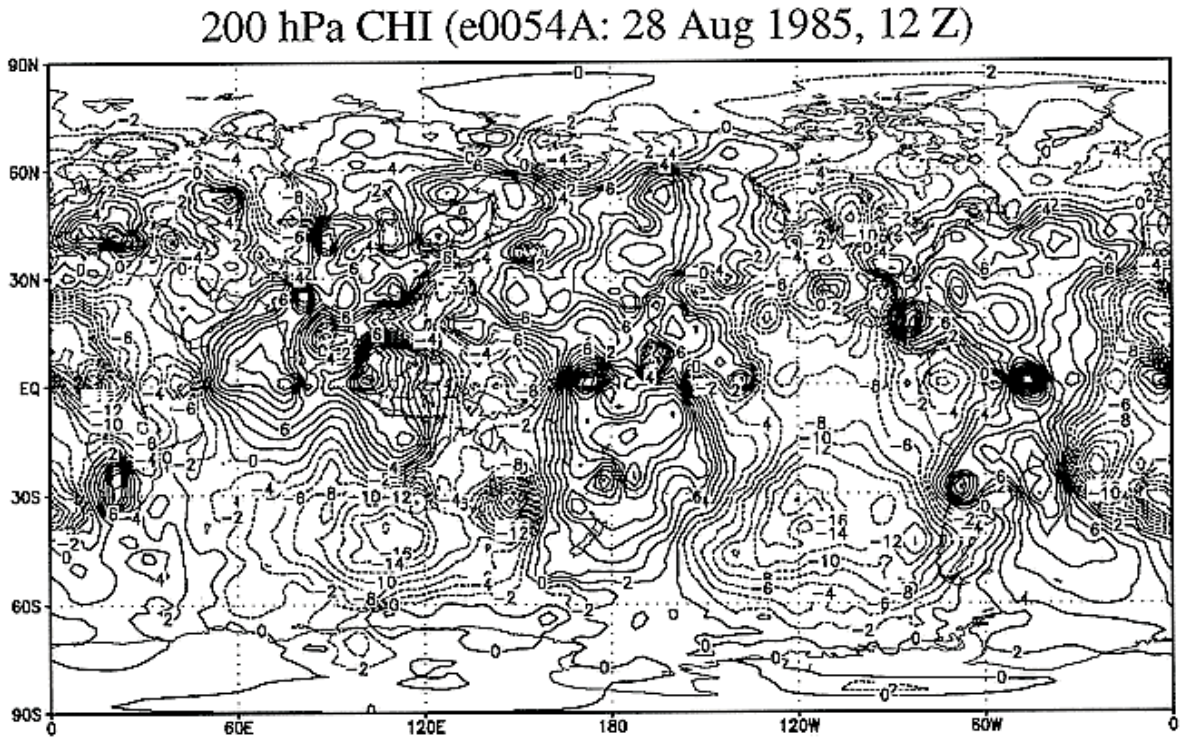

Fig. 6. Velocity potential analysis increments at 200 hPa for 1200 UTC 28 August 1985 (case 1) produced with PSAS (top panel) and GEOS-1 OI (bottom panel). Normalization is by the factor ($2\Omega \sin 45\ g^{-1}$), where Ω is the earth's rotation rate and g is the gravity constant. Contour interval: 2 m.

Cohn et al. (1998)

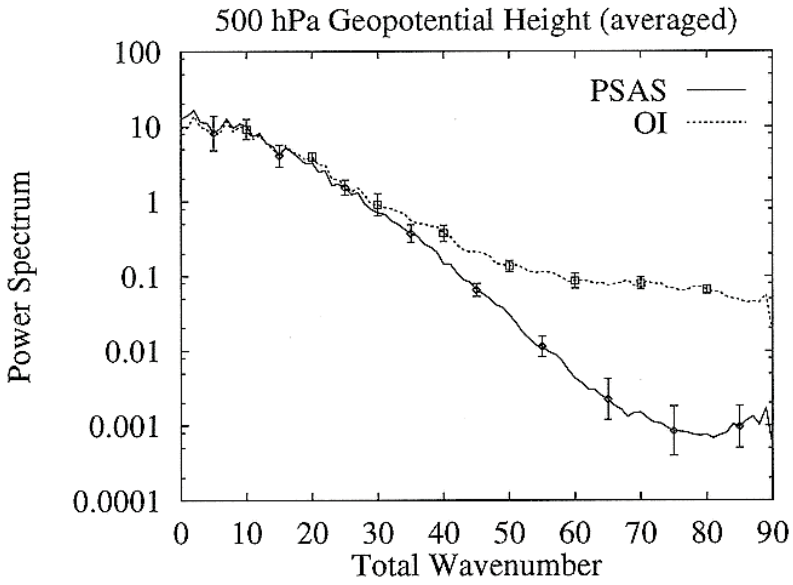

Fig. 3. Power spectra as a function of spherical harmonic total wavenumber for PSAS (solid line) and OI (dashed line) analysis increments of geopotential height at 500 hPa (five-case average, see Table 1). Bars indicate the range of the spectra among the five cases. Units: m^2.

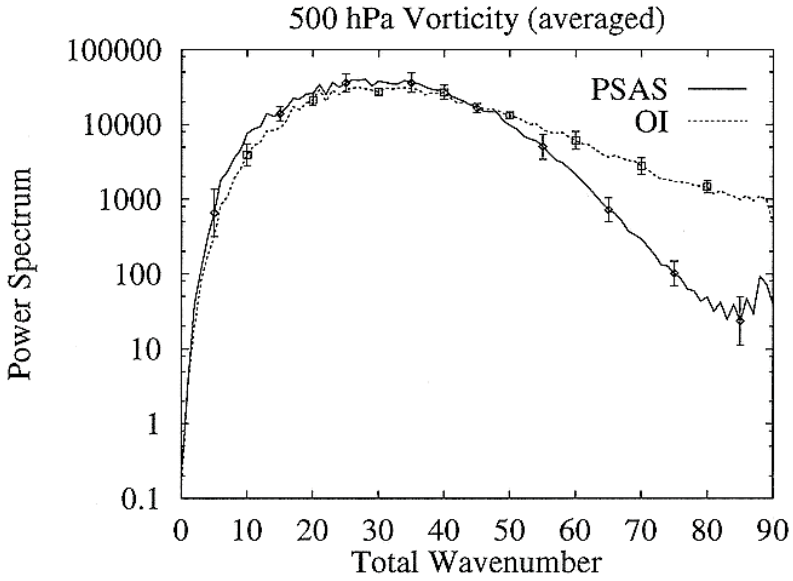

Fig. 4. As in Fig. 3 but for 500-hPa relative vorticity. Units: $10^{-15}s^{-2}$.

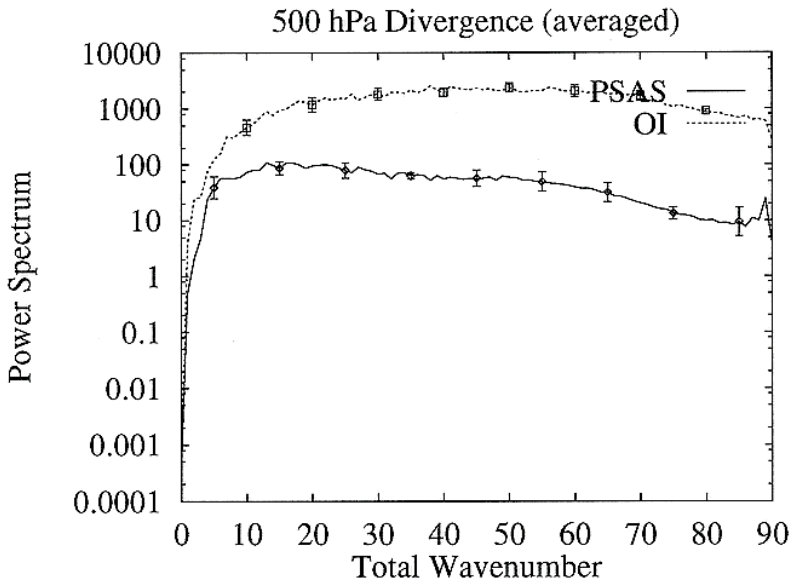

Fig. 5. As in Fig. 3 but for 500-hPa divergence. Units: $10^{-15}s^{-2}$.

Cohn et al. (1998)